

## NUMERICAL STUDY ON LIQUID DROPLET FORMATION IN T-JUNCTION MICROCHANNEL

Xiao-Bin Li, Juan-Cheng Yang, Feng-Chen Li†

School of Energy Science and Engineering, Harbin Institute of Technology, Harbin 150001, China  
[lifch@hit.edu.cn](mailto:lifch@hit.edu.cn)

### ABSTRACT

The formation of micro droplets involved a complex mechanism deriving from the competition between the interfacial tension, viscous shearing and other counterparts. In the present study, a volume-of-fluid (VOF) method within FLUENT software was used to study the droplet formation in a T-junction microchannel. By varying the velocity of continuous phase, we got droplet formation in “squeezing” process, and the shifting to “dripping” regime at a critical Capillary number. The pressure and velocity changing in both regimes were investigated in detail, supporting the result that the squeezing was dominated by the upstream pressure rising and the dripping was driven by shearing force. The numerical results hold a good agreement with the previously experimental measurements using confocal micro-PIV system. Furthermore, the motion inside an emerging droplet was also studied, showing intricate circulation flow.

### NOMENCLATURE

Ca	Capillary number
$D_h$	the droplet length
F	the source term owing to interfacial tension
$h$	the channel depth
P	local pressure
Q	flow rate
Re	Reynolds number
t	time of droplet generation
V	local velocity
$\vec{v}$	the velocity vector
w	the channel width

### Greek Letters

$\nabla$	the gradient of parameter
$\alpha$	the volume fraction
$\kappa$	the curvature of one phase
$\mu$	fluid viscosity

$\rho$	fluid density
$\sigma$	interfacial tension

### Subscript

c	the continuous phase
d	the dispersed phase
de	droplet detachment
$i$	$i=1,2$ , the first and the second phase
in	inlet direction
max	the maximum value
x	index of Cartesian coordinate

### INTRODUCTION

The microfluidic devices are often characterized by microchannels whose dimensions of width are typically around 100 microns, usually dealing with two or more different kinds of fluids at very low Reynolds numbers (Re). As a result of demand and development of microfabrication, pharmaceutical industry and biochemical application, etc., there is a growing interest in bubbles or droplets formation and precise control (for monosized emulsion) by using microfluidic devices [1-3], with many peculiar layouts of microchannels for bubble/droplet formation, breakup, fusion, mixing and sorting [4-5]. To generate continuous droplets' flow from a stream which is originally a continuous phase is such a process of how to pinch it off on demand, hereby one has to utilize counterpart of interfacial tension, by which the relatively stable interface and the surface of droplets are sustained. This counterpart could refer to shearing force in cross-flowing devices (T- or Y-shaped junction, sheath flowing) and co-flowing stream, or stretching force in elongational flow devices (flow focusing) [6]. The simple T-junction [7] and its derivate geometries have been used for droplets formation [8-9], fission [10-11] and fusion [4], where the complicated mechanism has been proposed by researchers with micro-PIV experiments [12-13] and numerical simulations [14-17]. However, for the droplets formation in T-junction, the dispersed phase is discretized by immiscible

† Corresponding author

continuous phase, it cannot be easily predicted by Capillary number (Ca, defined as the ratio of interfacial tension  $\sigma$  to shear stress by the continuous flow dynamic viscosity  $\mu_c$  and velocity  $u_c$ ) only because the diverse fluids, different operation conditions and varied geometries are involved. Therein, for Newtonian fluids system, the competition theory between viscous shearing and interfacial tension could make sense at moderate Capillary number, say shear-driven *dripping* regime [15]; in dripping regime, the droplet shape approaches to sphere, and its size doesn't show much change in a narrow Ca number range of  $4.0 \times 10^{-3} \sim 1 \times 10^{-2}$  [18]. At low Ca, the droplet shows bullet shape constrained by channel wall, and its size decreases with the increasing Capillary number; but it is almost independent of fluids' property (viscosity and interfacial tension), therefore this regime is not driven by shear stress, but pressure buildup upstream, say *squeezing* regime [15,18-19]. At higher Ca, a jet connected with the emerging droplet appears, lasts a long distance that times the channel width. This regime marches even downstream till the successive droplets generate, and say *jetting* regime [15]. When the viscoelastic fluid is introduced, a drops-on-a-string structure is observed [20], and the jetting phenomenon is advanced owing to extra intrinsic elasticity [21]. It is worth noting that the transition conditions from squeezing to dripping don't match in Capillary number in these experiments, even just for Newtonian cases. That may stem from the distinct operating conditions like velocity difference between continuous phase and dispersed phase, imposed pressure, gravity (for bubble creation), fluids' properties like viscosity contrast, density contrast, interfacial effect, geometrical design like aspect ratio, diameter of dispersed phase intrusion pore, and also surface effect like wettability (contact angle). For instance, if the diameter of dispersed phase intrusion pore is small enough, the dispersed phase will not approach the opposite channel wall, hence forming laminar flow side-by-side with continuous flow at low Ca; and it is explained by Nisisako that this laminar pattern is mainly driven by the gradient of interfacial tension at the head of the monomer flow [9]. Therefore, a scaling relation for the prediction of droplet size is also proposed by Garstecki et al. [19], in which the velocity contrast and approximate aspect ratio are covered. Further, the width ratio of T-junction is also developed in a physical model by Christopher et al., which captures several trends which are observed in their experiments, including squeezing-to-dripping transition [22]. However, the viscosity contrast isn't contained in scaling model, which may be ignored because viscosity ratio influences the droplet size only when the viscosities are comparable [22].

Besides, available simulations for bubble/droplet generation have also been performed by researchers using modern CFD methods (FLUENT package). Qian and Lawal (2006) conducted over 100 sets of simulations for Taylor slug flow; their dimensionless correlations for slug length accorded acceptably with all simulation data, and showed the interfacial tension and wall adhesion moderately impacted the slug lengths [23]. Based on 3D VOF (Volume of Fluid) numerical model, Sang et al. (2009) deduced an analytical model to predict the

droplet size in Newtonian and Non-Newtonian systems considering the viscosity effect [24], and the results agreed well with the experiments of Nisisako et al. [8] and Husny and Cooper-White [20]. Guo and Chen (2009) also simulated Taylor bubble flow by using VOF model to illuminate squeezing and shearing regimes which were similar to squeezing and dripping regimes for droplet generation [25]. Moreover, lattice Boltzmann method (LBM) was also proven to be a valid tool for droplet creation and deformation at microsacle [14].

However, there are still few cases of simulation for liquid/liquid droplet generation in microfluidic geometries. Since VOF method is very useful for two-phase flow with sharp interface reconstruction, here we adopt the VOF model within FLUENT package to capture the information of droplets formation. The properties of two immiscible fluids used are silicone oil (KF-6001) and water/glycerin solution [18], which have similar densities but large viscosity contrast; so we don't need concern the viscosity effect for bubble/droplet emerging. Since the choice of fluids is fixed, in need of a comparison with experimental work [18], we simply vary the Ca number to illuminate the evolution process and related regimes, changing the flow rate of continuous phase while setting that of dispersed phase constant.

## NUMERICAL MODEL AND VALIDATIONS

### The Mathematic/Geometric Model

The numerical model includes the continuity equation and Navier-Stokes (N-S) equation, which is still valid in currently microchannel environment; and a source term correlated with interfacial tension based on the continuum surface force (CSF) [26] is added to it. In this source term, the VOF model is tightly connected, i.e., in a computational cell, the density and the viscosity of the two-phase mixture read as:

$$\rho = \alpha_1 \rho_1 + \alpha_2 \rho_2$$

$$\mu = \alpha_1 \mu_1 + \alpha_2 \mu_2$$

where  $\alpha_i, \rho_i, \mu_i$  ( $i = 1, 2$ ) are the volume fraction, density and viscosity of the first and second phases, respectively. The volume fraction of first phase can be obtained by solving continuity equation for volume fraction:

$$\frac{\partial \alpha_1}{\partial t} + \vec{v} \cdot \nabla \alpha_1 = 0$$

where  $\vec{v}$  is velocity vector in N-S equation, hence the source term reads as:

$$F = 2\sigma \frac{\rho \kappa_1 \nabla \alpha_1}{(\rho_1 + \rho_2)}$$

Therein,  $\sigma$  is the interfacial tension, and  $\kappa_1$  is curvature of first phase in the matrix of the second phase, which can be computed by the contact angle, with a value of 150 degree in simulations.

The geometric model is a three-dimensional T-junction, as shown in Fig. 1, with a uniform aspect ratio of  $w/h=100/60=1.67$ ; the computational cells are meshed with uniform hexahedral grid. The inlet A and B are fed with silicone oil and water/glycerin solution, respectively; all the operation

conditions is set to be the same as the experiments of Oishi et al. [18] except their aspect ratio is  $100/45=2.22$ .

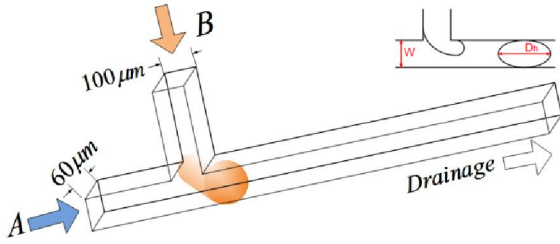


Fig. 1. The schematic diagram of geometric model. Inset, the droplet length and channel width.

### Validation with Micro-PIV Experiments

We have performed simulations with the superficial velocity of water/glycerin solution ( $\mu_1=7.46\text{mPa}\cdot\text{s}$ ) remaining at  $0.124\text{mm/s}$ , and silicone oil ( $\mu_2=44.1\text{mPa}\cdot\text{s}$ ) ranging from  $0.03$  to  $8.0\text{mm/s}$ , which covers the whole range of experiments by Oishi et al. [18]. The interfacial tension is set as  $11.1\text{mN/m}$ , so that the Capillary number varies from  $1.2\times 10^{-4}$  to  $3.2\times 10^{-2}$ . Under the above conditions, both squeezing and dripping regimes are observed, holding good agreement with experiments, showing in Fig. 2.

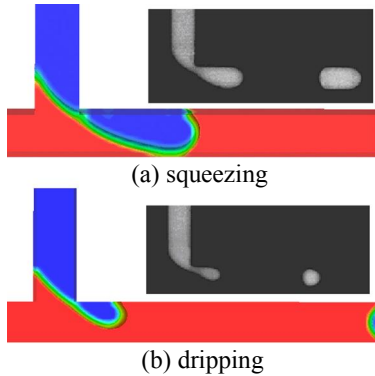


Fig. 2. The squeezing and dripping regimes. The insets are from Oishi et al. [18].

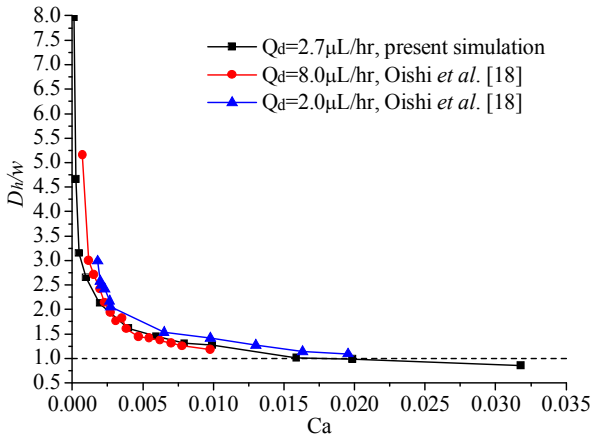


Fig. 3. Dimensionless droplet size as a function of Ca number.

To obtain the relationship between Ca number and droplet size, a non-dimensional droplet shape parameter, which is defined by the ratio of droplet length  $D_d$  to channel width  $w$ , is introduced (see inset in Fig. 1). When the parameter  $D_d/w$  exceeds 1, the emerging droplet will clog the main channel and attach the wall, restricting the droplet into slug shape. In Fig. 3  $D_d/w$  as a function of Ca together with the results of Oishi et al. [18] is shown, and they coincide well. From this figure we can find an inflection point is about  $Ca=4.0\times 10^{-3}$ , after which the ratio  $D_d/w$  comes to a plateau state. However, at this inflection point the ratio  $D_d/w$  is still larger than 1, and this will be explained later. If  $D_d/w\leq 1$ , the formation process is generally in the dripping regime, with large Ca number, and the droplet appears as sphere.

## RESULTS AND DISCUSSION

### Mechanism for Droplet Creation

According to the recent work of Garstecki et al. [19], Christopher et al. [22], De Menech et al. [15] and Oishi et al. [18], the mechanism of droplet formation should be classified into three regimes determined by the Ca numbers, namely squeezing, dripping and jetting. In the present work, the former two regimes are simulated.

Intuitively, the different regimes can be identified by the droplets' shape. The droplet confined by the channel wall appears as a slug at low continuous velocity (the dispersed phase is set unvaried), relating to small Ca number. Fig. 4 shows the evolution process of slug-shaped droplet formation. As the dispersed phase intrudes the junction area, its tip sustains as smooth as arc under the effect of interfacial tension, gradually it attaches the lower wall, and marches downstream. Later, the interface between the two immiscible fluids forms a neck, which comes to rupture and shrink to the junction corner and finally tears off.

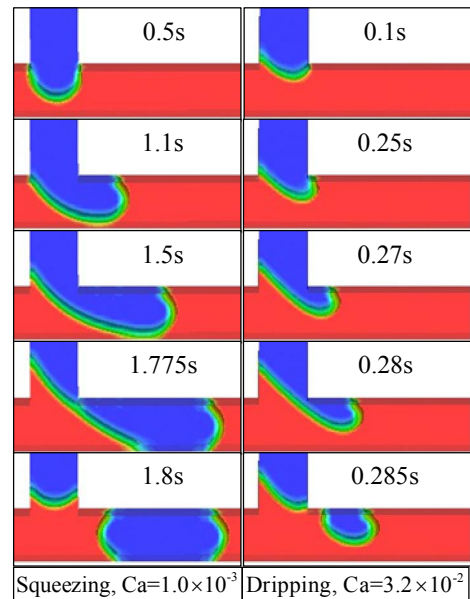


Fig. 4. The droplet formation process under two regimes.

In this process, the shearing effect is not large enough to pinch the neck off as a result of low velocity, therefore there should be another counterpart to force the droplet detach. De Menech et al. suggested this counterpart to interfacial tension is the pressure build-up upstream [15], which was proven by micro-PIV experiments by Oishi et al. [18]. Moreover, this result is in agreement with that the droplet size is independent of shearing force at low Ca [19]. Here we plot the vector field of velocity before the detachment, showing in Fig. 5. The velocity vectors indicate that the main flow direction of continuous phase is perpendicular to the neck arc, only small part of fluid flows near and along the wall, and form a vortex close to the boundary. Since the primary force is from the main flow, it pushes the dispersed phase to the junction corner. Therefore, the main stream works as squeezing effect.

For high velocity of continuous phase, the shearing force is the primary effect for the neck-pinching process. The formation of droplet shows the similar behavior with squeezing regime, i.e., tip intrusion → arc interface → neck shrinks → tears off (Fig. 4); however, the droplet creation is quick, i.e., time for droplet detachment decreases as Ca grows.

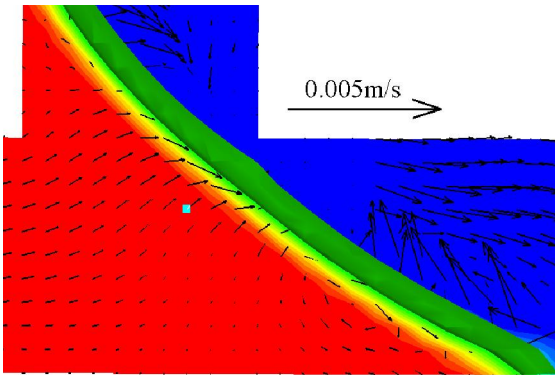


Fig. 5. The velocity profile at  $Ca=1.0 \times 10^{-3}$ ,  $t=1.775s$ .

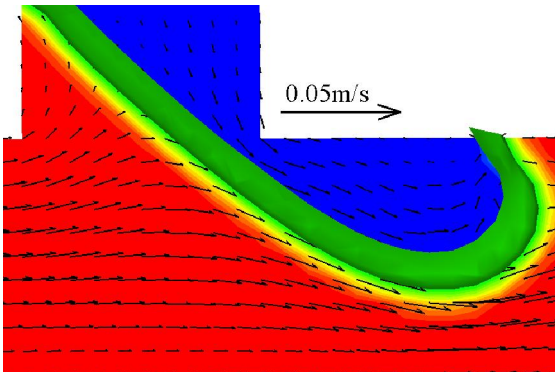
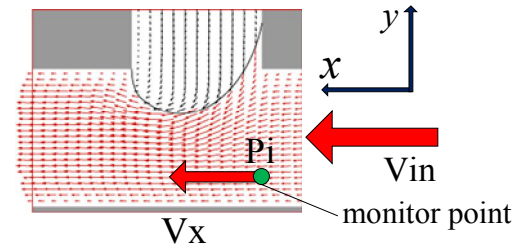


Fig. 6. The velocity profile at  $Ca=3.2 \times 10^{-2}$ ,  $t=0.28s$ .

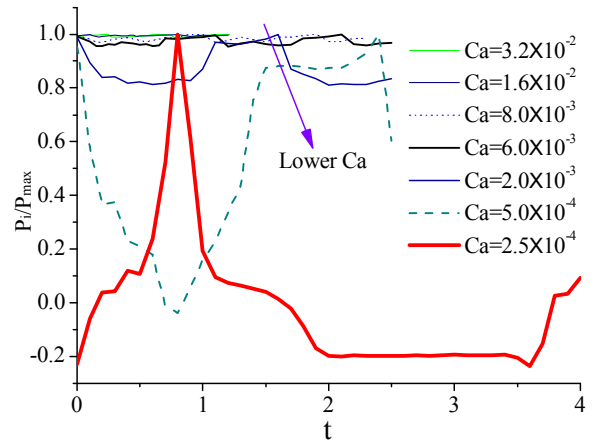
The vector field for high velocity is also displayed in Fig. 6. There is good distribution of velocity field in continuous phase that the main stream of continuous phase flow along the interface; the dimension of vectors is more uniform than that in Fig. 5, and they almost all orient to the same direction (marked as x axis, in Fig. 7A), resulting in high shear along the

interface. Therefore at this dripping regime, the droplet formation is mainly shear-driven.

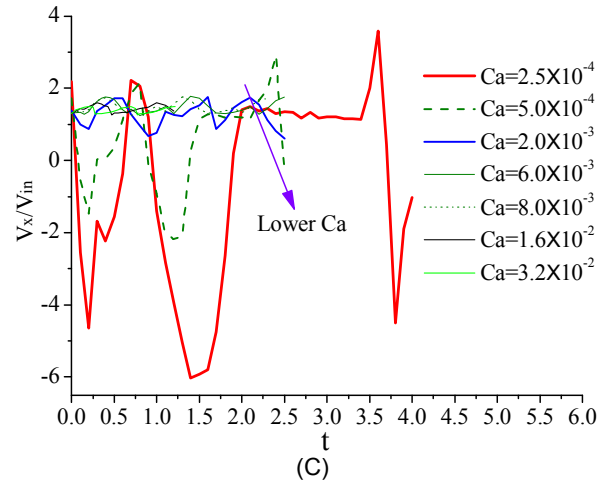
To verify this mechanism, we display the pressure and velocity changing during the generation process for a large range of Ca number, see Fig. 7(B, C). The data of pressure and velocity are extracted from the position just before the junction, which is marked as green point in Fig. 7(A). The monitor point is a little close to the lower wall, with a distance of  $20\mu m$  off, where the local velocity and pressure vary periodically.



(A)



(B)



(C)

Fig. 7. The pressure and velocity vary as time marching, (A), the monitor position; (B), the local pressure fluctuation which is normalized by maximum pressure in a droplet-generation period; (C), the local velocity fluctuation which is normalized by inlet velocity of continuous phase.

Every time, when the droplet generates, it will be carried into the main channel, and occupies the space of continuous flow, which makes the local pressure and velocity change periodically with a certain frequency; it also reveals that the fluctuations of local pressure and velocity are intrinsically connected. When Ca number grows higher, the amplitude of pressure fluctuation gets lower, but the frequency becomes higher; the corresponding curves become flatter compared with the cases of small Ca. That means the local pressure doesn't change significantly, the droplet creation at the junction has little effect when it propagates to the boundary of lower wall. For small Ca number, the pressure oscillates considerably, however, the frequency decreases. Also it clearly shows that the local velocity holds the same trends, and there is no negative value for large Ca, supporting the results in Fig. 5 and 6, i.e., high shear makes the continuous flow field uniform.

For the dispersed phase, there exists circular motion inside the tips of emerging droplets in both regimes. This is because the droplet has a continuous interface, and the friction between the two phases induces high shear. Moreover, the wall adhesion is a considerable factor in such microchannel, and the friction from both the channel wall and interface will bring out a circulation in the emerging droplets. A three-dimensional circulation was also observed inside an intact droplet experimentally by Kinoshita et al. [12].

#### Transition Point to Dripping Regime

As aforementioned, the inflection point ( $Ca=4.0 \times 10^{-3}$ ) shows that the decrease of non-dimensional length of droplet becomes slowly. Thereafter the droplet size doesn't show much changes, and the emerged droplets still remain contact with channel wall till approach the point where the ratio  $D_H/w$  equals 1.0, and which happens at  $Ca=1.6 \times 10^{-2}$  in our simulation.

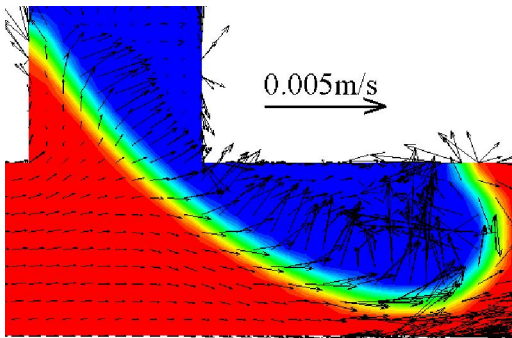


Fig. 8. The velocity profile at  $Ca=4.0 \times 10^{-3}$ ,  $t=4.555s$ , the fourth droplet as show in fig. 9 is in detaching.

Here we plot the field of velocity vector at the inflection point, as shown in Fig. 8. On the one hand, it can be seen that the emerging droplet doesn't contact the lower channel wall before the very moment of detaching because of the higher shear near the wall boundary (but the generated droplet does contact the channel wall). On the other hand, the velocity field shows a bit stronger shearing at interface, which means the shearing force becomes important.

However, it must be noticed that the pressure still plays an important role for droplet creation (Fig. 7). To verify the pressure effect, the pressure profile along the x axis ( $x=0$  corresponds to the inlet of continuous phase, and the junction position begins at 0.0003 on x axis) is shown in Fig. 9, in which the pulses of pressure indicate the droplet positions (marked by 1st, 2nd, etc.). There is a large difference in local pressure before the droplet detaching and after generating, and the pressure drop always exists at the two sides of droplet, as long as the formation process sets in. Once the droplet completely generates, the local pressure will jump high; therefore, as the droplets flow downstream, the pressure upstream will accumulate to a higher level.

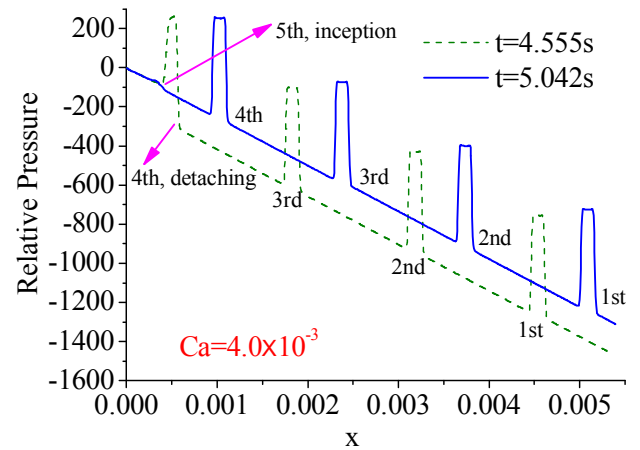


Fig. 9. The pressure profile along the streamwise direction.

Based on the previous discussions, we believe this inflection point is not exactly the transition point from squeezing regime to dripping regime, because both shearing force and ascending pressure affect the droplet formation. Therefore, it is necessary to suggest a criterion to distinguish them. If setting an upper limit of the perturbation of local velocity or pressure, e.g. less than 5%, hereby we can state the formation process is in dripping regime, which is dominantly driven by shearing. So the transition point in the present simulation is at  $Ca=1.6 \times 10^{-2}$ .

It is worth noting that the plateau of droplet size variation curve as shown in fig. 3 is clearly distinct to the unbounded flow like co-flowing condition [27], in which the constrained wall facilitates the droplet creation, i.e., as a result of the pressure rising that derived from the thin film between dispersed phase and the wall (the lubrication theory [28]).

#### Time for Droplet Detachment

When one intact droplet just generates, the next one is coming from the intrusion pore, and experiences the same route. After the successive one appears, we calculate this time interval as the droplet detachment time. As mentioned above, the droplet formation time decreases as the velocity of continuous phase grows, however, we cannot extract a scaling law for it just now, since the detachment time is influenced by many factors, like flow rate ratio, geometric aspect ratio and

viscosity ratio etc. A detailed discussion can refer to Garstecki et al. [19].

### Droplet Formation at Higher Ca Number

As the experiments [8] and numerical simulations [15] reported, there is a jetting regime exists at higher Ca number. However, in our 3D simulation we were not able to simulate this regime because the simulation is time-consuming due to its strict requirement of numerical resolution.

Nevertheless, in our previous 2D simulation, we have observed this regime, as shown in Fig. 10. The dimension of 2D model is twice that in 3D case, and the working fluids remain identical. The velocities for the continuous phase and dispersed phase are set as 0.03m/s and 0.02m/s, respectively, and the Capillary number is 0.12.

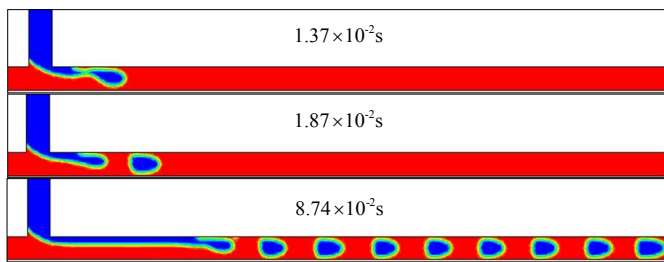


Fig. 10. The jetting regime in a 2D simulation domain.

It can be seen that the successive breakup point moves downstream, taking on a pattern of jet parallel to the continuous phase. We believe that jetting is an interface instability since the formed jet is almost stable and progressively travels. If the simulation cells are long enough for its growth, it may last as long as possible, till the channel is filled by the side-by-side flow. As a matter of fact, in the experiments of Nisisako et al. [6], the jet stops in the expansion pocket where the only flow pattern is the polydispersed droplets, generating in a disorderly fashion. Therefore, for its further understanding, one can refer to the review literatures of Stone (1994) [29] and Eggers (1995) [30].

### CONCLUSIONS

A study on droplet formation based on VOF model with FLUENT package is performed, where the effect of the local pressure and shearing force countering interfacial tension are investigated in detail. As interfacial tension behaving like a thin film with elasticity, and always trying to minimize its surface area, hereby it forms an interface between two immiscible fluid phase.

To shrink and rupture the interface the flow will come to different regimes as the flow condition changes. For squeezing regime at low Ca, once the emerging droplet attaches the lower wall, the continuous flow will be suddenly stacked, and even form the vortex flow. In a period of droplet generation, it will result in very large fluctuations of local velocity and pressure. For dripping regime, the shearing force prevails, and the pressure fluctuation is low; hence the deceleration of continuous flow will not happen, and accordingly the velocity fluctuation in streamwise direction also decreases. At higher

Ca, interface instability appears, along with a jetting flow, and the droplet generates further downstream.

It is noteworthy that Capillary number is primarily defined for continuous phase if the interfacial tension between two immiscible fluids is given since the fluids are fixed. So at a given Ca, the change of flow rate ratio  $Q_d/Q_c$  may significantly affect the droplet formation process, which needs a further study in the future.

### ACKNOWLEDGMENTS

This study was supported by National Natural Science Foundation of China (Grant No. 10872060) and Program for New Century Excellent Talents in University of China (Grant No. NCET-07-0235). The authors would thank H.-N. Zhang and W.-H. Cai of Complex Flow and Heat Transfer Lab (CFHTL) for valuable discussions and comments.

### REFERENCES

- [1] Stone, H. A., Stroock, A. D., and Ajdari, A. (2004). "Engineering flows in small devices: microfluidic towards a Lab-on-a-Chip." *Annu. Rev. Fluid Mech.*, 36, pp.381-411
- [2] Squires, T. M., and Quake, S. R. (2005). "Microfluidics: Fluid physics at the nanoliter scale." *Rev. Mod. Phys.*, 77, pp.977-1026
- [3] Teh, S. Y., Lin, R., Hung, L. H., and Lee, A. P. (2008). "Droplet microfluidics." *Lab Chip*, 8, pp.198-220.
- [4] Tan, Y. C., Fisher, J. S., Lee, A. I., Cristini, V., and Lee, A. P. (2004). "Design of microfluidic channel geometries for the control of droplet volume, chemical concentration, and sorting." *Lab Chip*, 4, pp.292-298.
- [5] Song, H., Chen, D. L., and Ismagilov, R. F. (2006). "Reactions in Droplets in Microfluidic Channels." *Angew. Chem. Int. Ed.*, 45, pp.7336-7356
- [6] Christopher, G. F., and Anna, S. L. (2007). "Microfluidic methods for generating continuous droplet streams." *J. Phys. D: Appl. Phys.*, 40, pp.R319-R336.
- [7] Thorsen, T., Roberts, R. W., Arnold, F. A., and Quake, S. R. (2001). "Dynamic pattern formation in a vesicle-generating microfluidic device." *Phys. Rev. Lett.*, 86, pp.4163-4166.
- [8] Nisisako, T., Torii, T., and Higuchi, T. (2002). "Droplet formation in a microchannel network." *Lab Chip*, 2, pp.24-26.
- [9] Nisisako, T., Torii, T., and Higuchi, T. (2004). "Novel microreactors for functional polymer beads." *Chem. Eng. J.*, 101, pp.23-29.
- [10] Link, D. R., Anna, S. L., Weitz, D. A., and Stone, H. A. (2004). "Geometrically mediated breakup of drops in microfluidic devices." *Phys. Rev. Lett.*, 92, pp.054503(4).
- [11] De Menech, M. (2006). "Modeling of droplet breakup in a microfluidic T-shaped junction with a phase-field model." *Phys. Rev. E*, 73, pp.031505(9).
- [12] Kinoshita, H., Kaneda, S., Fujii, T., and Oshima, M. (2007). "Three-dimensional measurement and visualization

- of internal flow of a moving droplet using micro-PIV.” *Lab Chip*, 7, pp.338-346.
- [13] Van Steijn, V., Kreutzer, M. T., and Kleijn, C. R. (2007). “ $\mu$ -PIV study of the formation of segmented flow in microfluidic T-junctions.” *Chem. Eng. Sci.*, 62, pp.7505-7514.
- [14] Van der Graaf, S., Nisisako, T., Schroën, C. G. P. H., Van der Sman, R. G. M., and Boom, R. M. (2006). “Lattice Boltzmann simulations of droplet formation in a T-shaped microchannel.” *Langmuir*, 22, pp.4144-4152.
- [15] De Menech, M., Garstecki, P., Jousse, F., and Stone, H. A. (2008). “Transition from squeezing to dripping in a microfluidic T-shaped junction.” *J. Fluid Mech.*, 595, pp.141-161.
- [16] Chandorkar, A., and Palit, S. (2009). “Simulation of droplet dynamics and mixing in microfluidic devices using a VOF-based method.” *Sensors & Transducers J.*, 7, pp.136-149
- [17] Liow, J. L. (2004). “Numerical simulation of drop formation in a T-shaped microchannel.” *15th Australasian Fluid Mechanics Conference, Sydney*
- [18] Oishi, M., Kinoshita, H., Fujii, T., and Oshima, M. (2009). “Investigation of droplet formation mechanism in micro T-shaped junction using confocal micro-PIV measurement.” *10th International Conference on Fluid Control, Measurement, and Visualization, FLUCOME, Moscow*
- [19] Garstecki, P., Fuerstman, M. J., Stone, H. A., and Whitesides, G. M. (2006). “Formation of droplets and bubbles in a microfluidic T-junction---scaling and mechanism of breakup.” *Lab Chip*, 6, pp.437-446.
- [20] Husny, J., and Cooper-White, J. J. (2006). “The effect of elasticity on drop creation in T-shaped microchannels.” *J. Non-Newtonian Fluid Mech.*, 137, pp.121-136.
- [21] Li, X.-B., Li, F.-C., Kinoshita, H., Oishi, M., and Oshima M. (2010). “Formation of Uniform Plugs and Monodispersed Droplets for Viscoelastic Fluid Flow in Microchannels.” *Earth & Space 2010 Conference, Hawaii*
- [22] Christopher, G. F., Noharuddin, N. N., Taylor, J. A., and Anna, S. L. (2008). “Experimental observations of the squeezing-to-dripping transition in T-shaped microfluidic junctions.” *Phys. Rev. E*, 78, pp.036317(12).
- [23] Qian, D., and Lawal, A. (2006). “Numerical study on gas and liquid slugs for Taylor flow in a T-junction microchannel.” *Chem. Eng. Sci.*, 61, pp.7609 – 7625.
- [24] Sang, L., Hong, Y., and Wang, F. (2009). “Investigatin of viscosity effect on droplet formation in T-shaped microchannels by numerical and analytical methods.” *Microfluid. Nanofluid.*, 6, pp.621-635.
- [25] Guo, F., and Chen, B. (2009). “Numerical Study on Taylor Bubble Formation in a Micro-channel T-Junction Using VOF Method” *Microgravity Sci. Technol.*, 21, pp.S51–S58.
- [26] Brackbill, J. U., Kothe, D. B., and Zemach, C. (1992). “A continuum method for modeling surface tension.” *J. Comput. Phys.*, 100, pp.335-354.
- [27] Cramer, C., Fischer, P., and Windhab, E. J. (2004). “Dropformation in a co-flowing ambient fluid.” *Chem. Eng. Sci.*, 59, pp.3045-3058.
- [28] Stone, H. A. (2005). “On lubrication flows in geometries with zero local curvature.” *Chem. Eng. Sci.*, 60, pp.4838-4845.
- [29] Stone, H. A. (1994). “Dynamics of drop deformation and breakup in viscous fluids.” *Annu. Rev. Fluid Mech.*, 26, pp.65-102.
- [30] Eggers, J. (1995). “Theory of drop formation.” *Phys. Fluids*, 7, pp.941-953.